Macromolecules
ARTICLE

Macromolecules **2009**, *42*, 8725–8732 **8725**
DOI: 10.1021/ma9017313

Mechanistic Investigation of the Silane, Germane, and Stannane Behavior When Incorporated in Type I and Type II Photoinitiators of Polymerization in Aerated Media

Mohamad El-Roz,* Jacques Lalevée,* Xavier Allonas, and Jean Pierre Fouassier

Department of Photochemistry, CNRS, University of Haute Alsace, Ecole Nationale Supérieure de Chimie de Mulhouse, 3 rue Alfred Werner, 68093 Mulhouse Cedex, France

Received August 3, 2009; Revised Manuscript Received September 14, 2009

ABSTRACT: The role of silanes, germanes, and stannanes R_3XH as co-initiators and additives to overcome the oxygen inhibition usually encountered in photopolymerization reactions in aerated media is demonstrated in experimental conditions where both a low light intensity and thin and low-viscosity samples are used. These results concerned with silanes as co-initiators are compared to data previously obtained in more viscous media where a lower effect of oxygen is expected. The striking role of R_3XH here is their use as additives in both type I and II photoinitiating systems. It allows to dramatically increase the polymerization rates and the final monomer conversions in the above-selected conditions. The mechanisms investigated by laser flash photolysis (LFP) and electron spin resonance (ESR) experiments are discussed.

Introduction

In the past few years, free radical photopolymerization (FRP) has attracted special attention due to its strong use in the UV radiation curing area. The selection of appropriate photoinitiators (PI) is of particular importance.[1,2] The design of high-performance PIs has been largely achieved using cleavable PI (type I) and two-component PI (type II). The addition of a third or a fourth compound to type II systems has already led to various more efficient three- or four-component PI; the incorporation of an additive into a type I PI remains, however, a fascinating challenge as no significant improvement has been reported so far in terms of rate of polymerization and conversion (see e.g. refs 1 and 2).

In FRP, a strong drawback concerns the well-known oxygen inhibition (Scheme 1).[1−4] Indeed, excited states are quenched by O_2. Both the initiating and propagating radicals are scavenged by O_2 and yield highly stable peroxyl radicals which cannot participate in any further polymerization initiation reactions.[5,6] The oxygen/radical interaction is a nearly diffusion-controlled reaction:[7] the polymerization only starts when oxygen is consumed.[8] In highly viscous or thick samples, the reoxygenation process is quite slow, leading to an efficient polymerization after an inhibition period. On the opposite, in very low viscosity or thin samples, the reoxygenation remains efficient, leading to strongly reduced monomer conversions; moreover, the lower the light intensity, the lower the initial O_2 consumption.

In the present paper, the main idea is to search for suitable additives in type I and type II PIs for the design of photoinitiating systems being able to work in aerated low-viscosity monomer media. We recently proposed new photoinitiating radicals based on silyl or germyl radicals ($R_3Si^•$, $R_3Ge^•$).[9,10] The high reactivity of $R_3Si^•$—generated from Si−Si bond containing systems (type I) or photoinitiator/silane combinations (type II)—toward the addition process to acrylate double bonds has been evidenced; the polymerization efficiency for a viscous epoxy acrylate matrix (Ebecryl 605 ∼14 500 cP) in aerated media has been explained on the basis of the specific behavior of the silyl radicals (a similar behavior was observed with $R_3Ge^•$).[9−11] We will mostly investigate here the photopolymerization of trimethylolpropane triacrylate TMPTA (viscosity ∼ 70−100 cP) under air and upon low light intensity using the silanes (germanes and stannanes) R_3XH shown in Scheme 2 as additives in type I (2,2′-dimethoxy-2-phenylacetophenone (DMPA), phenylbis(2,4,6-trimethylbenzoyl)phosphine oxide (BAPO), 2-hydroxy-2-methyl-1-phenyl propanone (HMP), and bis(cyclopentadienyl)bis[2,6-difluoro-3-(1-pyrryl)phenyl]titanium (Ti)) and type II (benzophenone (BP), isopropylthioxanthone (ITX), camphorquinone (CQ) and eosin Y (Eo) in the presence of an amine) photoinitiators. This will allow to illustrate the remarkable role of the $X^•$ ($R_3Si^•$, $R_3Ge^•$, and $R_3Sn^•$) radical chemistry in UV and visible light-induced FRP. The comparative role of R_3XH as co-initiators in a fluid and a viscous matrix will also be outlined. Lastly, the excited-state processes and the involved mechanisms investigated by laser flash photolysis (LFP) and electron spin resonance (ESR) experiments will be discussed.

Experimental Part

i. Compounds. The compounds reported in Scheme 2—diphenylsilane (**a**) tris(trimethylsilyl)silane (**b**), triethylsilane (**c**), dimethylphenylsilane (**d**), 1,1,2,2-tetraphenydisilane (**e**), triphenylsilane (**f**), triphenylgermane (**g**), and triphenyltin hydride (**h**)—were obtained from Aldrich or Tokyo Chemical Industry TCI. Ethyldimethylaminobenzoate (EDB, Esacure EDB from Lamberti) was used as a reference amine co-initiator. Di-*tert*-butyl peroxide was obtained from Aldrich. Benzophenone (BP), isopropylthioxanthone (ITX), camphorquinone (CQ), and eosin Y (Eo) were used in type II systems (from Aldrich) and 2,2′-dimethoxyphenylacetophenone (DMPA from Aldrich), phenylbis(2,4,6-trimethylbenzoyl)phosphine oxide (BAPO from Ciba-Basel), 2-hydroxy-2-methyl-1-phenyl propanone (HMP from Ciba, Basel), and bis(cyclopentadienyl)bis[2,6-difluoro-3-(1-pyrryl)phenyl]titanium (Ti, Irgacure 784 from Ciba, Basel) as type I photoinitiators.

*Corresponding authors. E-mail: j.lalevee@uha.fr (J.L.); mohamad.el-roz@uha.fr (M.E.).

Published on Web 09/23/2009

ii. Photopolymerization Experiments. For film polymerization experiments at RT, a given PI was dissolved into TMPTA (trimethylolpropane triacrylate from Cytec). In order to get a good reproducibility, thin samples with low PI optical densities were used. These experimental conditions allow a good dissipation of the heat produced during the polymerization reaction and avoid any internal filter effects.[12] The 20 μm thick films (laminated or under air) deposited on a BaF_2 pellet were irradiated with the polychromatic light of a Xe−Hg lamp for BP, DMPA, and HMP (Hamamatsu, L8252, 150 W). For the experiments with BAPO and ITX, a filter has been added in order to select an irradiation at $\lambda = 365$ nm (for these compounds, these irradiation conditions ensure a high oxygen inhibition for the process). For the visible light polymerization (Ti, CQ, Eo), an irradiation with a filtered xenon lamp (Hamamatsu L8253, 150 W) was selected ($\lambda > 400$ nm).

The evolution of both the double bond (acrylate) and the Si−H function content was continuously followed by real-time FTIR spectroscopy (Nexus 870, Nicolet) at about 1650 and 2100 cm^{-1}, respectively.[12,13] The R_p quantities that refer to the maximum rates of the polymerization reaction were calculated as presented in refs 12 and 13.

iii. Laser Flash Photolysis Experiments. Nanosecond laser flash photolysis (LFP) experiments were carried out using a Q-switched nanosecond Nd/YAG laser ($\lambda_{exc} = 355$ nm, 9 ns pulses; energy reduced down to 10 mJ, from Powerlite 9010 Continuum). The analyzing system consists of a pulsed lamp, a monochromator, a fast photomultiplier, and a transient digitizer.[14]

iv. Kinetic ESR Experiments. The kinetic ESR experiments carried out to determine the peroxyl/additive interaction rate constants have been performed on a X-band spectrometer (MS 200 Magnettech) as presented in ref 11.

v. DFT Calculations. All the calculations were performed using the hybrid functional B3LYP from the Gaussian 03 suite of program. Reactants and products were fully optimized at the B3LYP/6-31G* level (and frequency checked). The bond dissociation energy corresponds to the energetic difference between the parent hydrogenated compound and the radical. This procedure has been presented in detail in ref 14.

Scheme 1

$$PI \rightarrow {}^{1,3}PI \rightarrow R'^{\bullet} \rightarrow R'\text{-}M_n^{\bullet}$$

$${}^{1,3}PI + O_2 \rightarrow \text{quenching}$$

$$R'^{\bullet} + O_2 \rightarrow R'\text{-}O_2^{\bullet}$$

$$R'\text{-}M_n^{\bullet} + O_2 \rightarrow R'\text{-}M_n\text{-}O_2^{\bullet}$$

Results and Discussion

1. Reactivity of the Silyl Radicals. Kinetic data on the R_3XH chemistry and the generated radicals $R_3X^{\bullet} = R_3Si^{\bullet}$, $R_3Ge^{\bullet}$, and $R_3Sn^{\bullet}$ are rather scarce.[15] As carried out in previous works,[15,16] the formation of the $R_3X^{\bullet}$ radicals

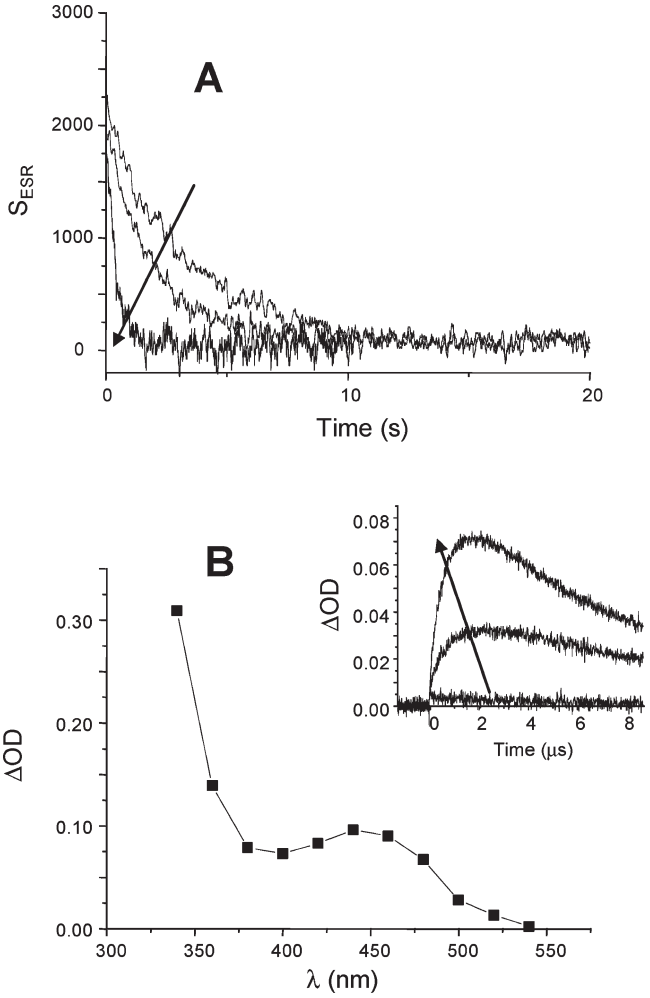

Figure 1. (A) Interaction of the *t*BuOO$^{\bullet}$ peroxyl radical with **e** (the experimental conditions are similar to ref 11). (B) UV/vis spectrum of the silyl radical of **e** in di-*tert*-butyl peroxide. Inset: kinetic traces at 340 nm in di-*tert*-butyl peroxide in the absence of **e** and upon addition of **e**.

Scheme 2

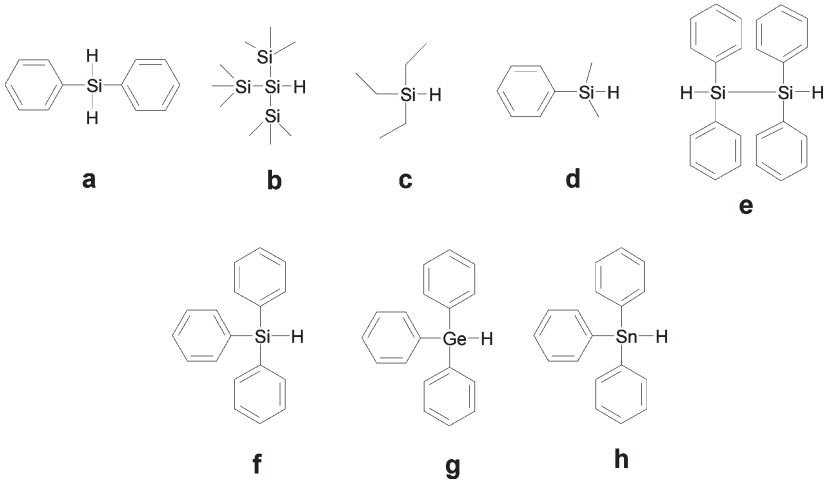

Table 1. Polymerization rates of TMPTA and Ebecryl 605 (Eb605) Using a BP/Co-initiator System (1%/1%, w/w)[a]

		BP[b,c]	*t*-Bu-O•[b]	*t*-Bu-OO•	Eb 605[b]	TMPTA	R•/MA
	BDE[d] (kcal/mol)	k_H (10^7 M^{-1} s^{-1})	$k_{H'}$ (10^7 M^{-1} s^{-1})	$k_{H''}$ (M^{-1} s^{-1})	$R_p/[M_0]$ × 100 (s^{-1})	$R_p/[M_0]$ × 100 (s^{-1})	k_{add} (10^7 M^{-1} s^{-1})
EDB	92.8	510 (1.0);	23	6	25.6	28.8 (8.1[e])	0.05
a	92.3	2.1 (0.55);	5.5	20	33.6	13.7	11
b	79.8	10 (0.95);	8.5	590	30.5	20.5	2.2
c	95.0	0.4 (0.65);	1.0	2.5	36.0	14.9	24
d	94.2	2.5 (0.65);	1.5	160	22.7	13.8	45
e	88.5	18 (0.75);	7.5	60		12.2	6.9
f	86.4	3.1 (0.75);	6.7	14	22.0	12.8	51
g	79.9	6.2 (0.69);	34	260	25.2	14.0	18
h	73.8	48 (0.74);	150	5200		15.5	4.8

[a] In laminate. I_0 = 44 mW cm^{-2}. Rate constants characterizing the formation and the reactivity of the radicals associated with the studied compounds. See text. [b] Reference 9d. [c] Ketyl radical quantum yields. [d] BDE at UB3LYP/6-31G* level (Gaussian 03). [e] Without co-initiator.

was investigated here through three different major pathways:

(a) The interaction of the *tert*-butoxyl radical (generated by photolysis of di-*tert*-butyl peroxide) with R_3XH yields the $R_3X^•$ radical whose absorption can be followed at about 300 nm: the risetime of this absorption allows the evaluation of the interaction rate constants by a usual Stern−Volmer treatment (Figure 1 and Table 1).

(b) The second way involves an interaction with a ketone triplet state (BP, ITX, ...) that leads to a hydrogen abstraction which generates a ketyl and a $R_3X^•$ radical. In that case, the ketyl radical of BP is easily observed at 545 nm. The observed rate constants as well as the ketyl radical quantum yields ($\phi_{K•}$), which are obviously equal to the $R_3X^•$ radical quantum yields, are given in Table 1.

(c) The interaction of R_3XH with a peroxyl radical also yields a $R_3X^•$ radical. This process is investigated by kinetic ESR (procedure presented in ref 11). The rate constants are gathered in Table 1 (Figure 1).

In these three interactions, an efficient hydrogen transfer occurs thereby demonstrating the high reactivity of the X−H function. The rate constants increase together with a decrease of the bond dissociation energy BDE(X−H) (Table 1). Particularly, tris(trimethylsilyl)silane (**b**) exhibits the best hydrogen-donating properties.

The direct observation of the $R_3X^•$ radicals by LFP provides a direct access to their reactivity. This was applied to their addition to methyl acrylate that is representative of the initiation process: the striking feature is that the k_{add} values are always very high (Table 1). These structures are clearly much better than the aminoalkyl radical of ethyldimethylaminobenzoate (EDB) which is already known as a very efficient polymerization initiating structure (k_{add} ~ 5×10^5 M^{-1} s^{-1}).[16]

2. Silane as Co-initiators. *a. Efficiency of BP/Silanes in a Fluid Matrix in Laminated Conditions*. In order to investigate the effect of the formulation viscosity on the reactivity of type II systems in laminated conditions, the photopolymerization of trimethylolpropane triacrylate (TMPA) as a fluid monomer has been carried out and explored in detail. For example, using BP/silane in TMPTA, a lower reactivity than that previously found in Ebecryl 605 is clearly noted (Table 1). Such a result is easily ascribed to the viscosity change. Indeed, in a rough approximation using the Stokes−Einstein equation for Ebecryl 605 and TMPTA, viscosities of 14 500 and 70−100 cP lead to diffusion rate constants about 4×10^5 and 9×10^7 M^{-1} s^{-1}, respectively.

In Ebecryl 605, all bimolecular rate constants will level off at about 4×10^5 M^{-1} s^{-1} whereas, in TMPTA, rate constants lower than 9×10^7 M^{-1} s^{-1} are discriminated. As a consequence, the triplet quenching (k_q) of BP by the monomer (TMPTA) appears in strong competition (k_H) with the hydrogen abstraction reaction (^{3}BP/silane) as shown in Scheme 3. For ^{3}BP/TMPTA, an interaction rate constant of 7×10^7 M^{-1} s^{-1} was found in ref 17. Taking into account the respective monomer and silane concentrations, the ^{3}BP/monomer interaction is expected as the major pathway (k_q[TMPTA] ~ 3×10^8 s^{-1} ≫ k_H[silane] ~ 5×10^5 s^{-1}). It is less important in ^{3}BP/EDB (k_H [EDB] ~ 4.5×10^6 s^{-1}). The k_H rate constants for the various ^{3}BP/silane couples range between 10^6 and 10^8 M^{-1} s^{-1}, which is lower than the diffusion rate constant in TMPTA. A similar behavior is found for germanes or stannanes.

Scheme 3

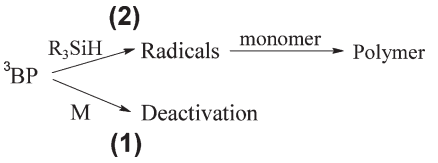

Contrary to TMPTA, in Ebecryl 605, the hydrogen abstraction can compete more with the triplet/monomer quenching. The ratio between the pathway (1) and (2) decreases (k_q[monomer] ~ 1×10^6 s^{-1} > k_H[silane] ~ 2×10^4 s^{-1} and = k_H[EDB] ~ 2×10^4 s^{-1}). As a consequence, the BP/silane systems are more efficient in Ebecryl 605. The reduced efficiency of silanes in TMPTA compared to EDB is explained by a decrease of the hydrogen abstraction yield. Interestingly, in TMPTA, the reactivity order of the different R_3XH is quite well correlated with k_H (Table 1). An enhanced reactivity is found compared to the other silanes for **b** which is characterized by the highest k_H (Table 1 and Figure 2).

*b. Efficiency of BP/Silane (**b**) in a Fluid Matrix under Air*. It has been previously reported that the BP/**b** system showed a higher efficiency (1.7 times) than the reference combination (BP/EDB) in the photopolymerization of Ebecryl 605 under air.[9d] Such a result is also observed in the TMPTA film (Figure 2) exposed to a low light intensity (44 mW cm^{-2}) where a significant effect of O_2 is expected. In contrast, when the irradiation intensity is increased (220 mW cm^{-2}), EDB is found more efficient (Figure 2). This is likely ascribed to the lower effect of oxygen at high intensity associated with a fast O_2 consumption by the aminoalkyl radicals. This demonstrates the interest of using a low light intensity to well evidence the interesting role of R_3XH on the oxygen inhibition.

3. Silanes as Additives for Type I and Type II Photoinitiator Systems in Fluid Matrix. *a. Type I System*. The additive effect of R_3XH (in particular **b**) in type I systems has been investigated for four well-known efficient photoinitiators (DMPA, BAPO, HMP, and Ti). Although they are characterized by a high reactivity, these PI are very sensitive to

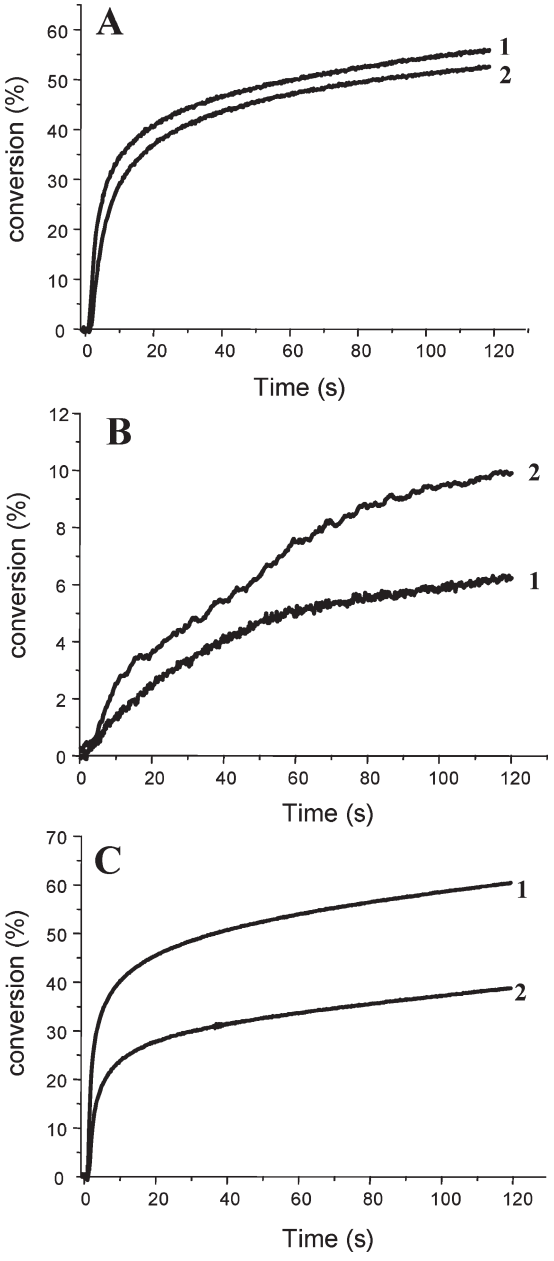

Figure 2. Conversion vs time curves for the laminated (A) and under air (B) photopolymerization of TMPTA. Photoinitiating system: BP/EDB (1) and BP/**b** (2) (1%/1% w/w). Hg−Xe lamp. I_0 = 44 mW cm^{-2}. Conversion vs time curves (C) upon a higher irradiation intensity under air (I_0 = 220 mW/cm^2).

oxygen in FRP. For example, despite a very efficient photopolymerization in laminated conditions, no polymerization is observed for Ti under visible light irradiation in our conditions. The results are reported in Figure 3. In DMPA, BAPO, and HMP, the radicals are generated from the cleavage of ^{3}PI according to reaction 1′ in Scheme 4; as known, these excited states are characterized by a short lifetime preventing their quenching by O_2 or monomer (reaction 3); for Ti, the Ti−C bond cleavage process is very fast[20] and undergoes the formation of radicals as demonstrated by spin trap ESR.[21] All these radicals either react with the monomer or are deactivated by oxygen to form peroxyl radicals. This oxygen quenching also occurs for the propagating radicals ($R'M_n^\bullet$) and efficiently competes in TMPTA with the propagation step (k_p[monomer] $\sim 3 \times 10^4$ s^{-1} < k_{O_2}[O_2] $\sim 2.1 \times 10^5$ s^{-1}). When nothing is added, an important R_p decrease is observed (as usually) as mainly peroxyl radicals are present in the time scale of the experiment. In contrast, the addition of R_3XH to the system is highly worthwhile as supported by the increase of both R_p/[M_0] and the final conversion which, e.g. for HMP, rises from 0.04 to 0.15 s^{-1} and 11% to 46% for [**b**] = 0 and [**b**] = 5%, respectively (Figure 3C).

The achieved performance can be explained through the reactions shown in Scheme 4 in the case of the ketone (type I)/silane systems. The same holds true if the silane is changed for a germane and a stannane. When using Ti, a polymerization is only noted in the presence of **b** (Figure 3). In that case, a fluorinated aryl and a cyclopentadienyl radical are generated and play the role of $R'^\bullet$ in Scheme 4.[21]

Silyl radicals are efficient to consume oxygen ($R_3Si^\bullet + O_2 \rightarrow R_3Si{-}O_2^\bullet$) as rate constants close to the diffusion limit ((2−3) × 10^9 M^{-1} s^{-1}) were measured by LFP.[9a] As seen in Table 1 for e.g. tris(trimethylsilyl)silane (**b**) where a hydrogen abstraction rate constant of 590 M^{-1} s^{-1} has been found by kinetic ESR (for Y = *t*Bu), an efficient peroxydation process regenerates an initiating silyl radical according to $Y{-}O_2^\bullet + R_3Si{-}H \rightarrow Y{-}O_2H + R_3Si^\bullet$ where Y stands for an initiating (R' or $R_3Si^\bullet$) or a propagating radical ($-M_n^\bullet$). This value is much higher than that found for amines (such as EDB: $k \sim 6$ M^{-1} s^{-1}; $tBuOO^\bullet + EDB \rightarrow tBuO_2H + EDB^\bullet$), in agreement with the better behavior of **b** in aerated conditions. Another interest of the silane-derived peroxyl radical is the possibility of a rearrangement reaction (reaction 6 in Scheme 4) recreating a silyl radical.[11,18] Under polychromatic irradiation, photodecomposition of the formed hydroperoxides Y−OOH occurs (reaction 7), and the generated radicals ($Y{-}O^\bullet$ and $OH^\bullet$) can abstract a hydrogen atom from a silane or directly initiate the polymerization process.

From Figure 3, it is worth noting that the improvement of the polymerization is connected with the hydrogen abstraction rate constant $k_{H''}$ of the $YOO^\bullet/R_3XH$ interaction reported in Table 1. This demonstrates that this process (reaction 4 in Scheme 4) is probably the fingerprint for the R_3XH effect. Figure 4 depicts the silane concentration effect. The reactivity of the DMPA/**b** system is strongly improved when [**b**] increases. A similar behavior is observed for HMP (Figure 3C). This is easily explained by an increase of the efficiency of the bimolecular reaction 4 compared to the other deactivation pathways of the peroxyls.

All these results outline the interest of R_3XH in type I PI where (i) the usually formed radicals $R'^\bullet$ are involved in the initiation process and (ii) R_3XH behaves as a high-performance additive to convert inefficient peroxyls into new additional efficient initiating $R_3X^\bullet$ radicals (reactions 4 and 5) and thereby to reduce the detrimental oxygen inhibition effect.

Interestingly, the final conversion increase (Δconv) at e.g. t = 120 s is well correlated with $k_{H''}$. This is also well exemplified by the decrease of the Si−H content (see below e.g. Si−H in Figure 4) throughout the polymerization reaction. As peroxyls are mainly present, the very high Si−H conversion is ascribed to reaction 4. Indeed, the reaction of the monomer radicals $RM_n^\bullet$ with **b** is assumed as quite low as rate constants k < 4 10^4 M^{-1} s^{-1} are determined (Figure 5) by following the decay of the acrylate radicals at different **b** concentrations using the procedure described in ref 19. Accordingly, in addition to the propagation step, the monomer radicals preferentially react with oxygen and not with the Si−H functions, and as a consequence, the peroxyls are responsible for the further Si−H conversion.

b. Type II System. Figure 6 shows the additive effect of **b** in BP/EDB for the polymerization of TMPTA under air. The

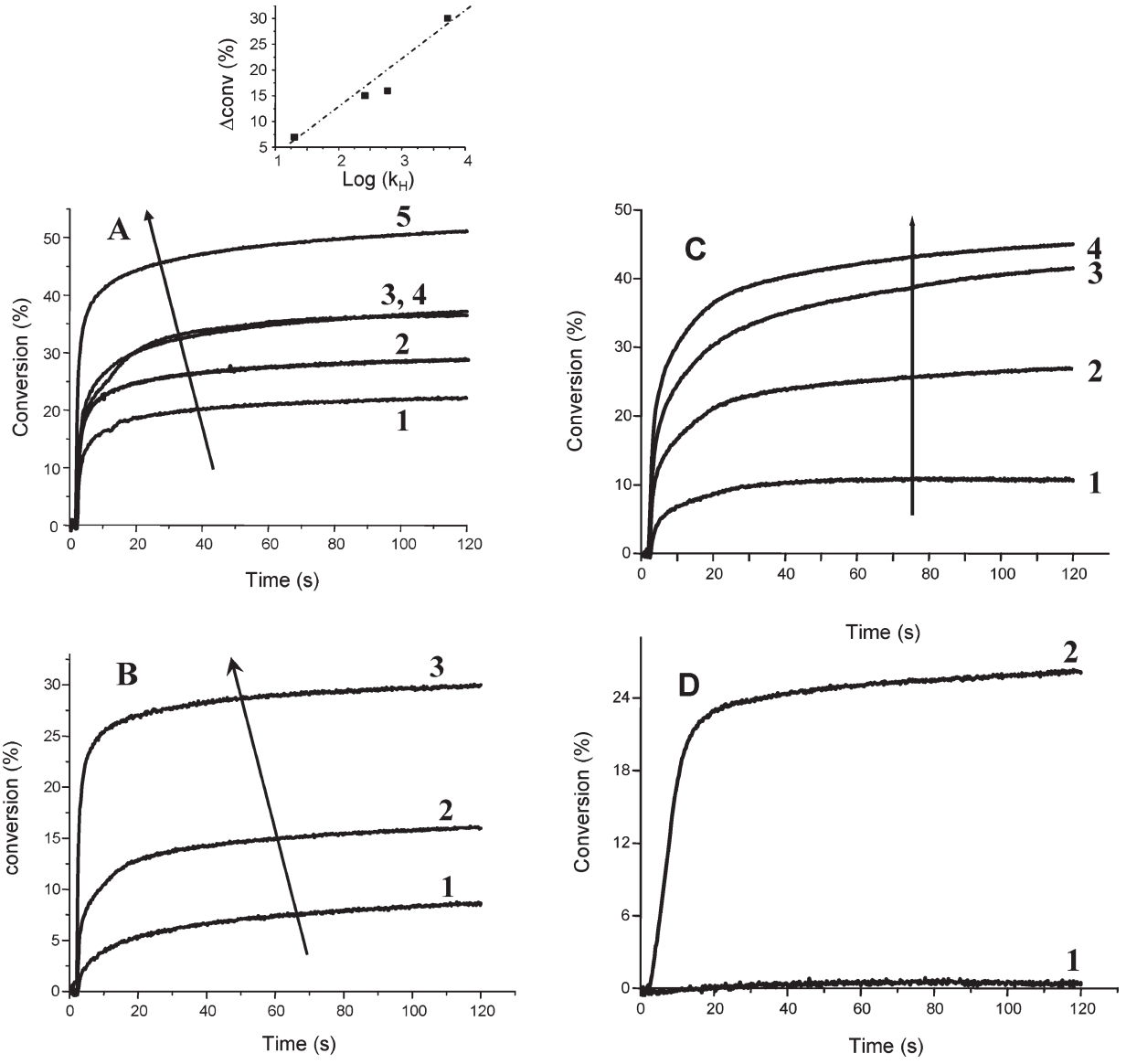

Figure 3. Conversion vs time curves for the photopolymerization of TMPTA under air as a function of the photoinitiator and the additive. (A) DMPA/additive (1%/3% w/w): (1) no additive; (2) **a**; (3) **g**; (4) **b**; (5) **h**. $I_0 = 22$ mW cm^{-2}; sample thickness = 20 μm. Inset: the conversion increase for different additive at $t = 120$ s (Δconv) vs the hydrogen abstraction rate constant (ROO$^\bullet$/R′3XH). (B) BAPO/additive (1%/3% w/w): (1) no additive; (2) **b**; (3) **h**. $I_0 = 3.5$ mW cm^{-2}; $\lambda_{exc} = 365$ nm; sample thickness = 20 μm. (C) HMP/additive (1%/x% w/w): (1) no additive; (2) **b** (1.5%); (3) **b** (3%); (4) **b** (5%). $I_0 = 22$ mW cm^{-2}; sample thickness = 20 μm. (D) Ti/additive (0.1%/3% w/w): (1) no additive; (2) **b**; $I_0 = 60$ mW cm^{-2}; xenon lamp; 300 nm $< \lambda <$ 800 nm; sample thickness = 20 μm.

Scheme 4

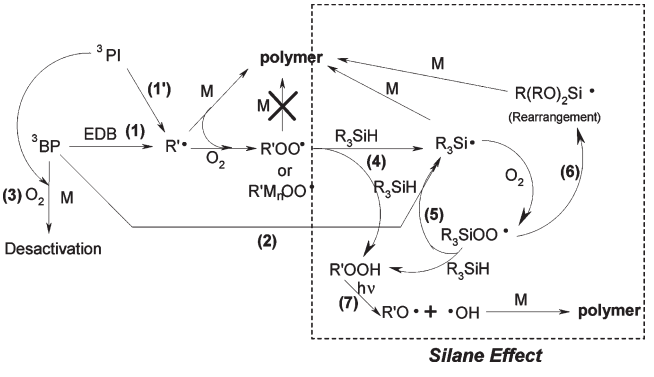

BP/EDB/**b** (1%/1%/2% w/w/w) system exhibits a significant enhanced reactivity compared to BP/EDB (1%/3% w/w) or BP/**b** (1%/3% w/w). It should be noted that the co-initiator molar concentration in BP/EDB is higher than for the BP/**b** system since the molecular weight of **b** > EDB. Interestingly, as found for type I system, a high conversion of the Si−H function is noted (Figure 6). This is also a strong evidence for the YOO$^\bullet$/silane interaction.

The positive effect is also explained on the basis of Scheme 4 for the ketone (type II)/silane systems, in full agreement with the data obtained in type I systems. However, in the present case, a hydrogen abstraction between the triplet excited state and R_3XH can also occur (reaction 2). According to this scheme, a competition between the reactions 1−3 can be predicted. From the diffusion and interaction rate constants, it is expected that the monomer quenching represents the major process (k_q[TMPTA] $\sim 3 \times 10^8 \gg k_H$[EDB] $\sim 4.5 \times 10^6 > k_H$[$R_3SiH$] $\sim 1 \times 10^6 > k_{O_2}$[$O_2$] $\sim 2 \times 10^5$ s^{-1}). The hydrogen abstraction from the amine is more favorable than from R_3XH. The polymerization rate using BP/**b** reflects the specific behavior of R_3XH under air[9,10] (reactions 4−6).

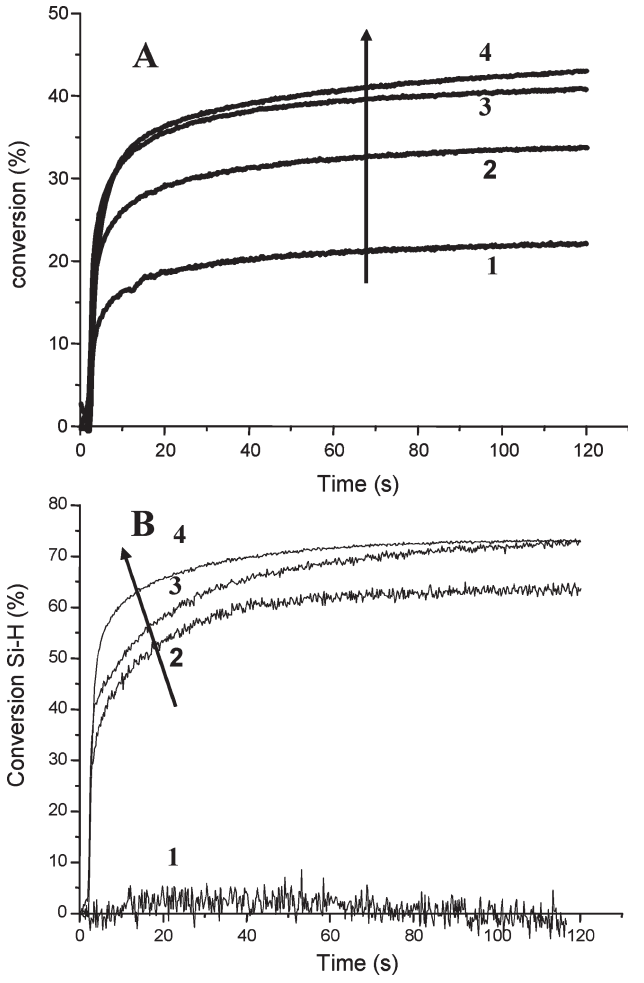

Figure 4. Conversion vs time curves for the photopolymerization of TMPTA under air as a function of the additive concentration. (A) DMPA/additive (**b**) (1%/*x*% w/w): (1) no additive; (2) **b** (3%); (3) **b** (6%); (4) **b** (10%) (I_0 = 22 mW cm^{-2}; sample thickness = 20 μm). (B) Conversion of the Si−H function vs time during the photopolymerization of TMPTA under air.

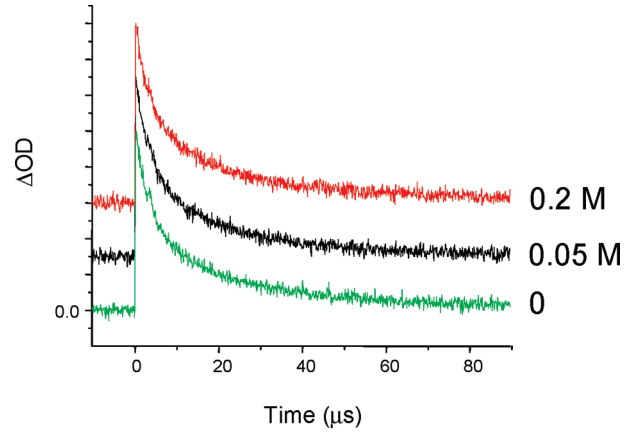

Figure 5. Observation of the acrylate radicals (derived from the addition of the aminoalkyl radical of triethylamine to methyl acrylate) at 480 nm according to the procedure described in ref 19 for different concentrations of **b**.

These results demonstrate the interest of the amine/R_3XH combination in type II PI where (i) EDB is used to get a high efficient hydrogen abstraction and favors the initiation

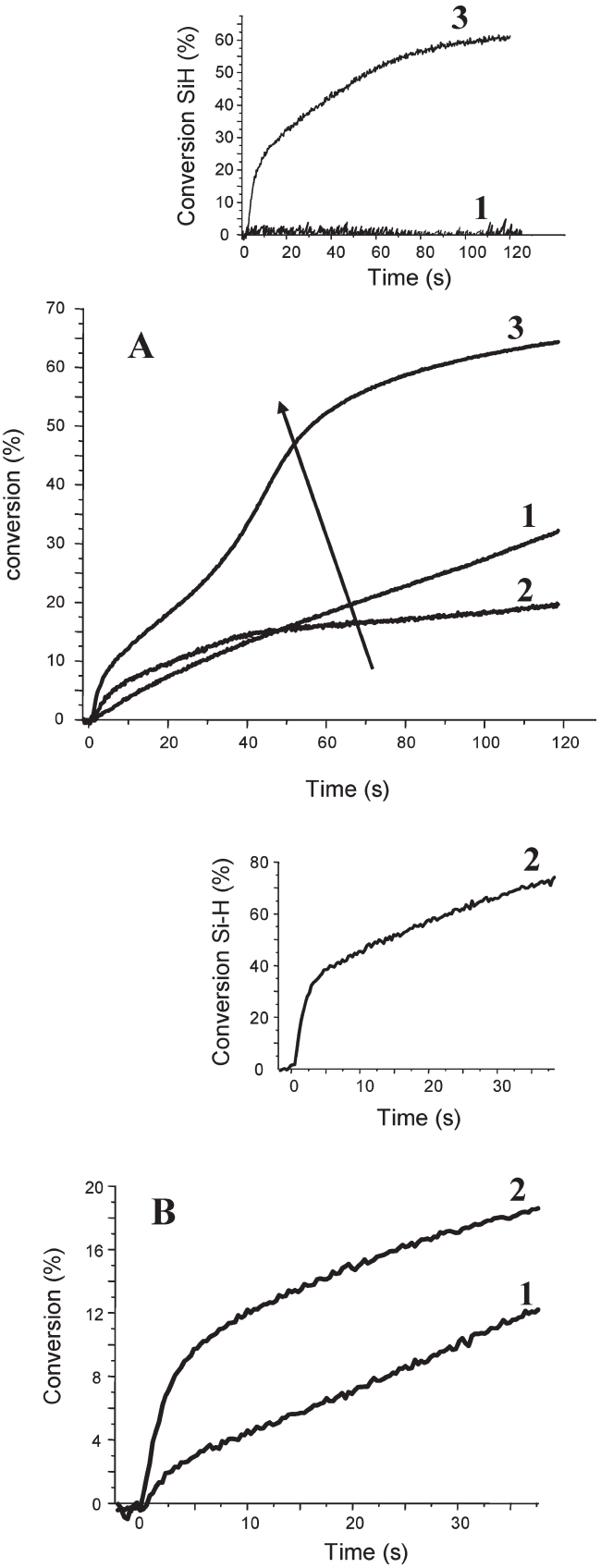

Figure 6. Conversion vs time curves for the photopolymerization of TMPTA under air. (A) BP/co-initiator with CoI (1%/*x*% w/w): (1) EDB 3%; (2) **b** 3%; (3) EDB/**b** (1%/2%). Inset: the conversion of Si−H function. I_0 = 44 mW cm−2; sample thickness = 20 μm. (B) ITX/CoI with CoI (w/w): (1) EDB 3%; (2) EDB/**b** (1%/2%). Inset: the conversion of the Si−H function. I_0 = 1 mW cm^{-2}; sample thickness = 20 μm.

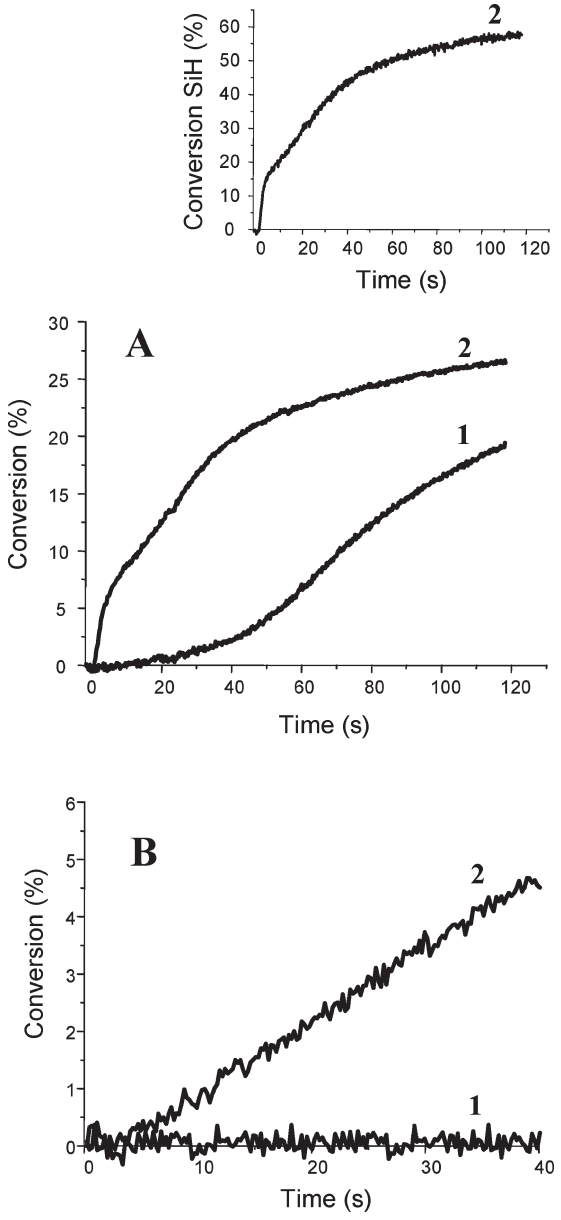

Figure 7. Conversion vs time curves for the photopolymerization of TMPTA under air. (A) CQ/co-initiator with CoI (3%/x% w/w): (1) EDB 3%; (2) EDB/**b** (1%/2%). Inset: conversion of the Si−H function. I_0 = 30 mW cm−2; xenon lamp; 400 nm < λ < 800 nm; sample thickness = 20 μm. (B) Eo/co-initiator (0.1%/x% w/w): (1) MDEA (methyldiethanolamine) 3%; (2) MDEA/**b** (1%/2%). I_0 = 60 mW cm^{-2}; xenon lamp; 400 nm < λ < 800 nm; sample thickness = 20 μm.

process and (ii) R_3XH behaves as a high performance additive as discussed above for type I PI.

Similar behaviors are also encountered for other type II photoinitiators (ITX, CQ, and Eo—with addition of R_3XH) being able to work upon UV or visible light irradiation (Figure 7). Scheme 4 also applies for ITX and CQ.

Conclusion

The effect of silanes, germanes, and stannanes as additives in type I and type II photoinitiators for FRP of TMPTA in aerated media and under low light intensity is reported. A huge improvement of the polymerization efficiency is noted. The reaction mechanisms are discussed and explain the role of oxygen. The increase of reactivity correlates well with the $YOO^{\bullet}/R_3Si-H$ hydrogen abstraction rate constants. The effect of the monomer matrix in photopolymerization reactions using R_3Si-H as co-initiators has also been compared in a high (Ebecryl 605) and a low-viscosity monomer (TMPTA). This work could be extended to other additives exhibiting a high reactivity with peroxyl radicals and a dual behavior (i.e., capable to work both as additive and co-initiator). Moreover, this general effect of R_3Si-H can be adapted for a large range of irradiation conditions. On the basis of preliminary findings, some positive effects are also expected in practical applications under a higher light intensity. For example, this should help to polymerize more efficiently low-viscosity monomers under air.

References and Notes

(1) (a) Pappas, S. P. *UV Curing: Science and Technology*; Technology Marketing Corp.: Aachen, 1985. (b) Dietliker, K. *A Compilation of Photoinitiators Commercially Available for UV Today*; Sita Technology Ltd.: Edinburgh, London, 2002.

(2) (a) Fouassier, J. P. *Photoinitiation, Photopolymerization and Photocuring: Fundamental and Applications*; Hanser Publishers: New York, 1995. (b) *Radiation Curing in Polymer Science and Technology*; Fouassier, J. P., Rabek, J. F., Eds.; Elsevier Science Publishers Ltd.: London, 1993. (c) *Photochemistry and UV curing: New Trends*, Fouassier, J. P., Ed.; Research Signpost: Trivandrum, 2006. (d) *Basics and Applications of Photopolymerization Reactions*; Fouassier, J. P., Allonas, X., Eds.; Research Signpost: Trivandrum, in press. (e) Fouassier, J. P.; Allonas, X.; Lalevée, J.; Dietlin, C. In *Handbook on Photochemistry and Photophysics of Polymer Materials*; Allen, N. S., Ed.; Wiley: New York, in press.

(3) Rabek, J. F. *Mechanisms of Photophysical Processes and Photochemical Reactions in Polymers. Theory and Applications*; Wiley-Interscience: Chichester, 1987.

(4) Gou, L.; Opheim, B.; Scranton, A. B. In *Photochemistry and UV Curing: New Trends*; Fouassier, J. P., Ed.; Research Signpost: Trivandrum, 2006.

(5) (a) Bolon, D. A.; Webb, K. K. *J. Appl. Polym. Sci.* **1978**, *9*, 2543–2552. (b) Wight, F. R. *J. Polym. Sci., Polym. Lett. Ed.* **1978**, *16*, 121–127. (c) Studer, K.; Decker, C.; Beck, E.; Schwalm, R. *Prog. Org. Coat.* **2003**, *48*, 101–111.(d) *Radiation Curing of Polymeric Materials*; ACS Symposium Series 417; Hoyle, C. E., Kinstle, J. F., Eds.; American Chemical Society: Washington, DC, 1989. (e) Hofer, M.; Moszner, N.; Liska, R. *J. Polym. Sci., Part A: Polym. Chem.* **2008**, *46*, 6916–6927. (f) Keskin, S.; Jockusch, S.; Turro, N. J.; Arsu, N. *Macromolecules* **2008**, *41*, 4631–4634.(g) Karasu, F.; Arsu, N.; Jockusch, S.; Turro, N. J. *Macromolecules* **2009**, Article ASAP, DOI: 10.1021/ma9008669. (h) Karaca Balta, D.; Arsu, N.; Yagci, Y.; Jockusch, S.; Turro, N. J. *Macromolecules* **2007**, *40*, 4138–4141.

(6) (a) Davidson, R. S. In *Radiation Curing in Polymer Science and Technology*; Fouassier, J. P., Rabek, J. F., Eds.; Elsevier Science Publishers Ltd.: London, 1993; Vol *III*.(b) Hoyle, C. E.; Kim, K. J. *J. Appl. Polym. Sci.* **2003**, *33*, 2985–2996. (c) Decker, C. *Makromol. Chem.* **1979**, *180*, 2027–2030.(d) Alfassi, Z. *Peroxyl Radicals*; Wiley-CH: Chichester, 1997.

(7) Maillard, B.; Ingold, K. U.; Scaiano, J. C. *J. Am. Chem. Soc.* **1983**, *105*, 5095–5099.

(8) (a) Hoyle, C. E.; Kim, K.-J. *J. Radiat. Curing* **1985**, 9–15. (b) Decker, C.; Jenkins, A. D. *Macromolecules* **1985**, *18*, 1241–1244.

(9) (a) Lalevée, J.; Allonas, X.; Fouassier, J. P. *J. Org. Chem.* **2007**, *72*, 6434–6439. (b) Lalevée, J.; El-Roz, M.; Allonas, X.; Fouassier, J. P. *Macromolecules* **2007**, *40*, 8527–8530. (c) Lalevée, J.; El-Roz; Allonas, X.; Fouassier, J. P. *J. Polym. Sci., Part A: Polym. Chem.* **2008**, *46*, 2008–2014. (d) Lalevée, J.; Dirani, A.; El-Roz, M.; Allonas, X.; Fouassier, J. P. *Macromolecules* **2008**, *41*, 2003–2010.

(10) Lalevée, J.; Blanchard, N.; El-Roz, M.; Graff, B.; Allonas, X.; Fouassier, J. P. *Macromolecules* **2008**, *41*, 4180–4186.

(11) Lalevée, J.; Blanchard, N.; Graff, B.; Allonas, X.; Fouassier, J. P. *J. Organomet. Chem.* **2008**, *693*, 3643–3649.

(12) (a) Lalevée, J.; Allonas, X.; Jradi, S.; Fouassier, J.-P. *Macromolecules* **2006**, *39*, 1872–1879. (b) El-Roz, M.; Lalevée, J.; Morlet-Savary, F.; Allonas, X.; Fouassier, J.-P. *J. Polym. Sci., Part A: Polym. Chem.* **2008**, *46*, 7369–7375.

(13) El-Roz, M.; Lalevée, J.; Allonas, X.; Fouassier, J.-P. *Macromol. Rapid Commun.* **2008**, *29*, 804–808.

(14) Lalevée, J.; Allonas, X.; Fouassier, J. P. *J. Am. Chem. Soc.* **2002**, *124*, 9613–9621.

(15) (a) Chatgilialoglu, C. *Organosilanes in Radical Chemistry*; Wiley: Chichester, 2004. (b) Chatgilialoglu, C.; Ingold, K. U.; Lusztyk, J.; Nazran, A. S.; Scaiano, J. C. *Organometallics* **1983**, *2*, 1332–1335. (c) Chatgilialoglu, C.; Scaiano, J. C.; Ingold, K. U. *Organometallics* **1982**, *1*, 466–469.
(16) Lalevée, J.; Graff, B.; Allonas, X.; Fouassier, J. P. *J. Phys. Chem. A* **2007**, *111*, 6991–6998.
(17) Lemee, V.; Burget, D.; Jacques, P.; Fouassier, J. P. *J. Polym. Sci., Part A: Polym. Chem.* **2000**, *38*, 1785–1794.
(18) Zaborovskiy, A. B.; Lutsyk, D. S.; Prystansky, R. E.; Kopylets, V. I.; Timokhin, V. I.; Chatgilialoglu, C. *J. Organomet. Chem.* **2004**, *689*, 2912–2919.
(19) Lalevée, J.; Allonas, X.; Fouassier, J. P. *Chem. Phys. Lett.* **2005**, *415*, 287–290.
(20) Klingert, B.; Roloff, A.; Urwyler, B.; Wirz, J. *Helv. Chim. Acta* **1988**, *71*, 1858–1867.
(21) Criqui, A.; Lalevée, J.; Allonas, X.; Fouassier, J. P. *Macromol. Chem. Phys.* **2008**, *209*, 2223–2231.